

# Structure and Reactivity of Aromatic Radical Cations Generated by FeCl<sub>3</sub>

Takahiro Horibe, Shuhei Ohmura, Kazuaki Ishihara\*

Graduate School of Engineering, Nagoya University, B2-3(611), Furo-cho, Chikusa, Nagoya 464-8603, Japan

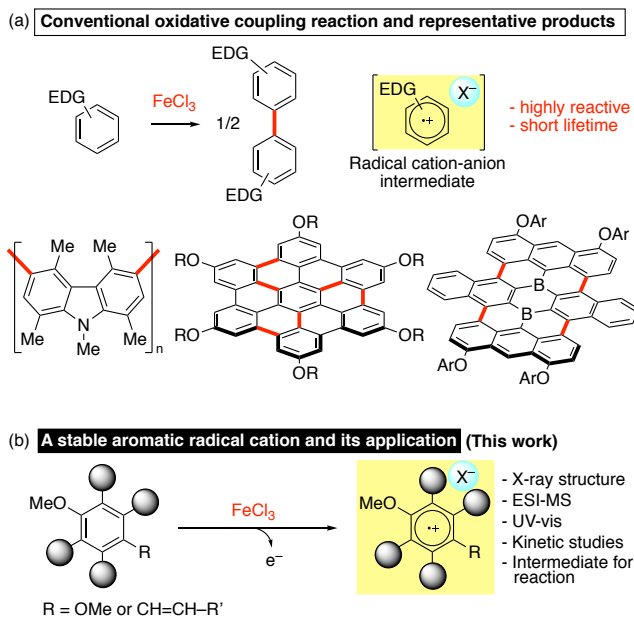
Supporting Information Placeholder

**ABSTRACT:** This paper describes the isolation and characterization of an aromatic radical cation generated by FeCl<sub>3</sub>. X-ray crystallographic analysis and kinetic studies reveal the mechanism of the generation of aromatic radical cation. In the solid state, a tight ion-pair of a radical cation with FeCl<sub>4</sub><sup>-</sup> is observed. Leveraging the efficient generation of the radical cation–FeCl<sub>4</sub><sup>-</sup> ion pair, we explore a radical cation-induced cycloaddition of *trans*-anethole initiated by catalytic amount of FeCl<sub>3</sub>. Both [4 + 2] cycloaddition and [2 + 2] cycloaddition with a broad substrate scope are also described. Moreover, a 100g-scale reaction is demonstrated with the use of 1 mol% of FeCl<sub>3</sub> as a simple and a highly active initiator.

Aromatic radical cations are open-shell reactive species that appear in various one-electron oxidation reactions.<sup>1</sup> Since radical cation-induced reactions exhibit reactivity and selectivity complementary to those in thermal reactions,<sup>2</sup> tremendous effort has been devoted to identifying radical cation-induced reactions. The explicit characterization of these key radical cation intermediates can serve as a basis for the discovery of further reactions. However, because of their high reactivities and short lifetimes, the structural characterization of radical cations has been challenging.<sup>3</sup> Within this catalytic regime, FeCl<sub>3</sub>-promoted oxidation reactions are of particular interest.<sup>4</sup> For examples, FeCl<sub>3</sub> has been shown to promote oxidative coupling reactions<sup>5,6</sup> and the Scholl reaction,<sup>7,8</sup> which have been utilized for syntheses of polycyclic aromatic hydrocarbons for more than a century (Scheme 1a). Despite its wide application for material science,<sup>9</sup> the mechanism of the FeCl<sub>3</sub>-promoted oxidation reaction has been scarcely studied. Whereas the oxidation reactions are believed to proceed through aromatic radical cations as a key intermediate,<sup>6a–e,10</sup> there have been no reports on the isolation of aromatic radical cations generated by FeCl<sub>3</sub>. Major challenges include a highly reactive and labile aromatic radical cation, which decomposes or undergoes oxidation reaction immediately.<sup>10,11</sup> Therefore, the actual structure of aromatic radical cations remains unclear. In particular, the identity of counteranion (X<sup>-</sup>) has remained elusive in key previous studies.

Here, we report the isolation and characterization of an aromatic radical cation–anion generated by FeCl<sub>3</sub> (Scheme 1b). Moreover, by means of the efficient generation of radical cation by FeCl<sub>3</sub>, we have developed radical cation-induced [4 + 2] cycloaddition as well as [2 + 2] cycloaddition promoted by catalytic amounts of FeCl<sub>3</sub>.

## Scheme 1. FeCl<sub>3</sub>-mediated Radical Cation Generation.



The isolation of an aromatic radical cation generated by FeCl<sub>3</sub> was approached empirically. Most of the electron-rich aromatics examined did not give isolable products. Fortunately, sterically congested arene **1** gave radical cation **2** in 84% yield in CH<sub>2</sub>Cl<sub>2</sub>/MeCN (Figure 1a). The X-ray crystal structure of **2** reveals an ion pair of FeCl<sub>4</sub><sup>-</sup> with **1**<sup>•+</sup> (Figure 1b). Additionally, **1**<sup>•+</sup> could be observed in solution by UV-vis spectroscopy ( $\lambda_{\text{max}} = 519 \text{ nm}, 483 \text{ nm}$ )<sup>12</sup> and ESI-MS analysis ( $m/z = 270.16$ ) under ambient conditions (Figures 1c and 1d). To elucidate the mechanism for the generation of **2**, kinetic studies were conducted for FeCl<sub>3</sub> and **1**. First-order dependency for FeCl<sub>3</sub> and zero-order dependency for **1** were observed (Figure 1e), which suggested that the nuclearity of the iron species was un-

changed between the ground state and rate-determining transition state. Combined with the known structure **A** of  $\text{FeCl}_3$  in MeCN,<sup>13</sup> we propose the overall mechanism for oxidation shown in Figure 1f. Namely, zero-order in **1** implies rate-limiting internal reorganization in the dimeric ground-state structure **A**, which we propose involves a ligand dissociation to afford  $\text{FeCl}_4^-$  and  $\text{FeCl}_2^+(\text{MeCN})_3$  (**B**).<sup>14</sup> This oxidant **B** is immediately scavenged by **1** to give **2**, thus exhibiting zero-order behavior. Because the zero-order behavior suggests that **1** is an efficient scavenger of **B**, this observation suggests that less kinetically reducing arenes could also be oxidized by  $\text{FeCl}_3$ -promoted oxidation in MeCN.

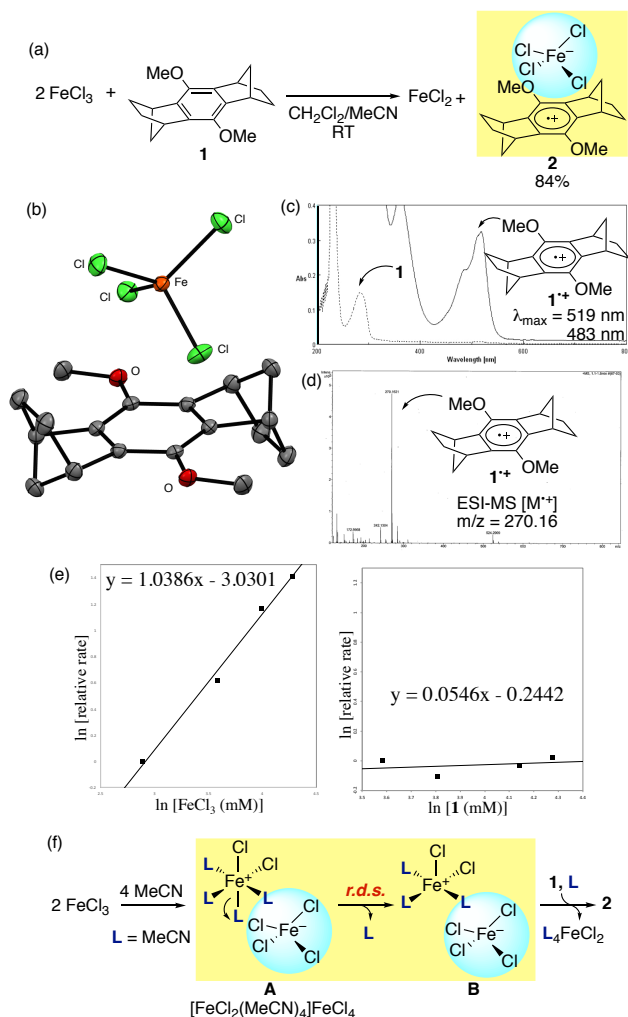
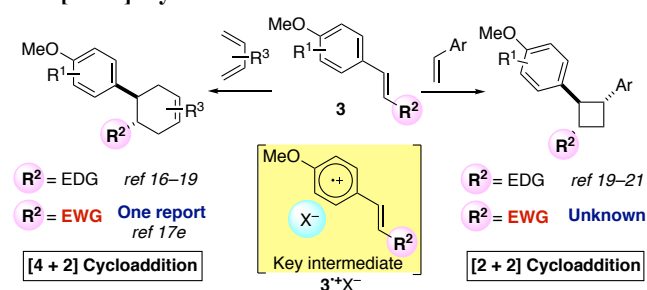


**Figure 1.** (a) The generation of radical cation **2** by  $\text{FeCl}_3$ . (b) Thermal-ellipsoid representation of **2** at the 50% probability level. Hydrogens have been omitted for clarity. (c) UV-vis spectrum of **2**. (d) ESI-MS spectrum for **2**. (e) Kinetic studies for  $\text{FeCl}_3$  and **1**. (f) The proposed mechanism for the generation of **2**.

With the oxidant **B** identified, we applied  $\text{FeCl}_3$ -promoted oxidation for a radical cation-induced cycloaddition. We were intrigued by [4 + 2] cycloaddition and [2 + 2] cycloaddition of *trans*-anethole **3** (Scheme 2). The key intermediate is  $3^{+\bullet}$ , which undergoes [4 + 2] cycloaddition with diene or [2 + 2] cycloaddition with styrene. To date,

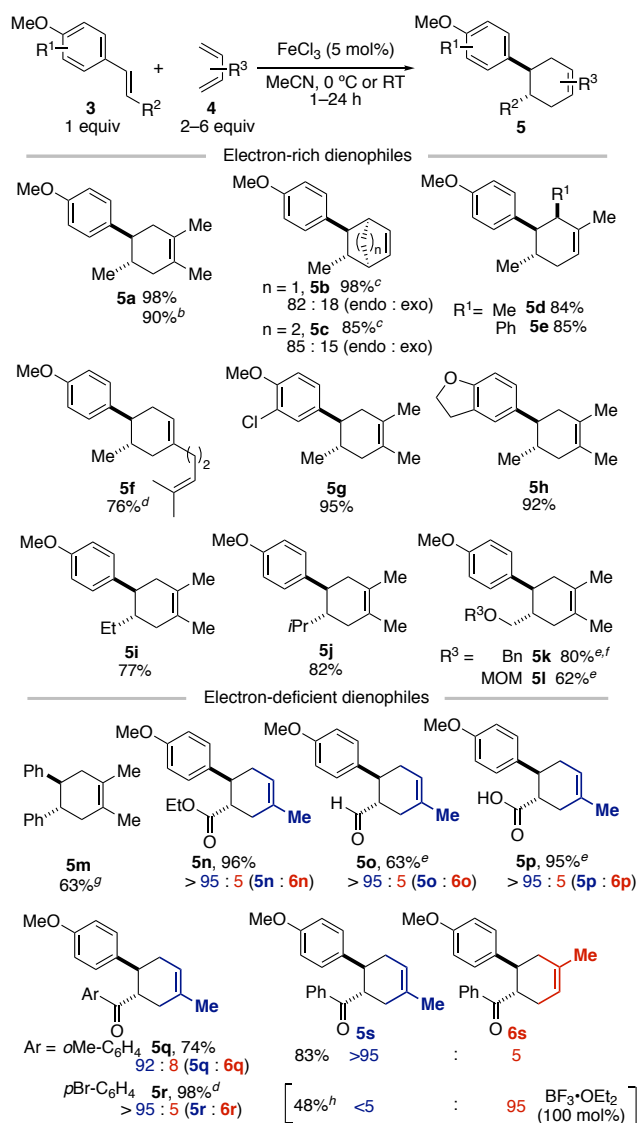
implementation of an initiator has been the primary strategy developed for the generation of  $3^{+\bullet}$ .<sup>15</sup> Great progress has been made employing aminium radical cation,<sup>16</sup> photoredox catalysis,<sup>17</sup> electrochemical methods<sup>18</sup> and iron(III) catalysis<sup>19</sup> for [4 + 2] cycloaddition. With regard to cross [2 + 2] cycloaddition, photoredox catalysis,<sup>20</sup> hypervalent iodine initiator<sup>21</sup> and iron(III) catalysis<sup>19</sup> have been developed. Whereas a broad substrate scope of both cycloadditions has been achieved, electron-deficient *trans*-anetholes (**3**) are less explored. For examples, only one report of electron-deficient **3** for [4 + 2] cycloaddition has appeared recently from Ferreira's group.<sup>17e</sup> Regarding [2 + 2] cycloaddition, there have been no examples of electron-deficient **3**.<sup>22</sup> The generation of electron-deficient  $3^{+\bullet}$  is more difficult because of the high oxidation potential of such substrates. To achieve a wide substrate scope including electron-deficient **3**, *in-situ* formed **B** as a strong oxidant should be suitable.

### Scheme 2. Previously Reported [4 + 2] Cycloaddition and [2 + 2] Cycloaddition.



Our studies in this area commenced with examination of  $\text{FeCl}_3$ -initiated [4 + 2] cycloaddition (Table 1). To our delight, 5 mol% of  $\text{FeCl}_3$  gave the corresponding product in 98% yield when **3a** was used (see **5a**). Interestingly, 5 mol% of isolated **2** also promoted the cycloaddition to give **5a** in 90% yield. Both cyclic and acyclic dienes gave the corresponding products in high yields (see **5b–5f**). Various aromatic groups and substituents of  $\beta$ -position of **3** were well tolerated (see **5g–5l**). Remarkably, our oxidation system was also suitable for electron-deficient dienophiles (**3m–3s**). In some cases, 5 mol% of  $\text{Fe}(\text{OTf})_3$  in place of  $\text{FeCl}_3$  was also effective (see **5k–5m**, **5o** and **5p**).<sup>23</sup> Presumably, higher oxidation potential of  $\text{Fe}(\text{OTf})_3$  facilitates the oxidation of such less-reducing substrates.<sup>24</sup> Whereas the conventional aminium radical cation give **5m** in only 30% yield,<sup>25</sup> iron(III) oxidation system afforded **5m** in an improved 63% yield. In the case of  $\alpha,\beta$ -unsaturated carbonyls, such as esters, aldehydes, carboxylic acids and ketones (**3n–3s**), the corresponding products (**5n–5s**) were obtained in high yield with high regioselectivity in 2–24 h. As in previous examples of radical cation cycloaddition, the regioselectivity of the corresponding products (**5n–5s**) is complementary to that of thermal [4 + 2] cycloadducts (**6n–6s**). Indeed, the opposite isomer **6s** was mainly obtained from  $\text{BF}_3 \cdot \text{OEt}_2$ -promoted [4 + 2] cycloaddition of **3s**. These results suggest that  $\text{FeCl}_3$  acts as a one-electron oxidant rather than a Lewis acid.

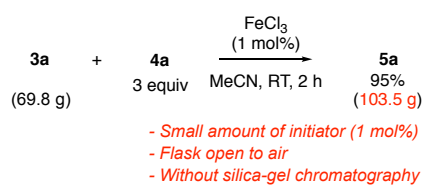
**Table 1. Scope of Radical Cation-induced [4 + 2] Cycloaddition.<sup>a</sup>**



<sup>a</sup>The reaction was carried out with FeCl<sub>3</sub> (5 mol %), **3** (1 equiv) and **4** (2–6 equiv) in MeCN at 0 °C or room temperature. <sup>b</sup>Using **2** (5 mol%) instead of FeCl<sub>3</sub>. <sup>c</sup>CH<sub>2</sub>Cl<sub>2</sub> was used as a solvent. <sup>d</sup>MeCN/CH<sub>2</sub>Cl<sub>2</sub> were used as solvents. <sup>e</sup>Using Fe(OTf)<sub>3</sub> (5 mol%) instead of FeCl<sub>3</sub>. <sup>f</sup>Using **4** (9 equiv). <sup>g</sup>Using Fe(OTf)<sub>3</sub> (10 mol%) instead of FeCl<sub>3</sub>. <sup>h</sup>The reaction was carried out with BF<sub>3</sub>·OEt<sub>2</sub> (100 mol %), **3** (1 equiv) and **4** (10 equiv) in Et<sub>2</sub>O at room temperature.

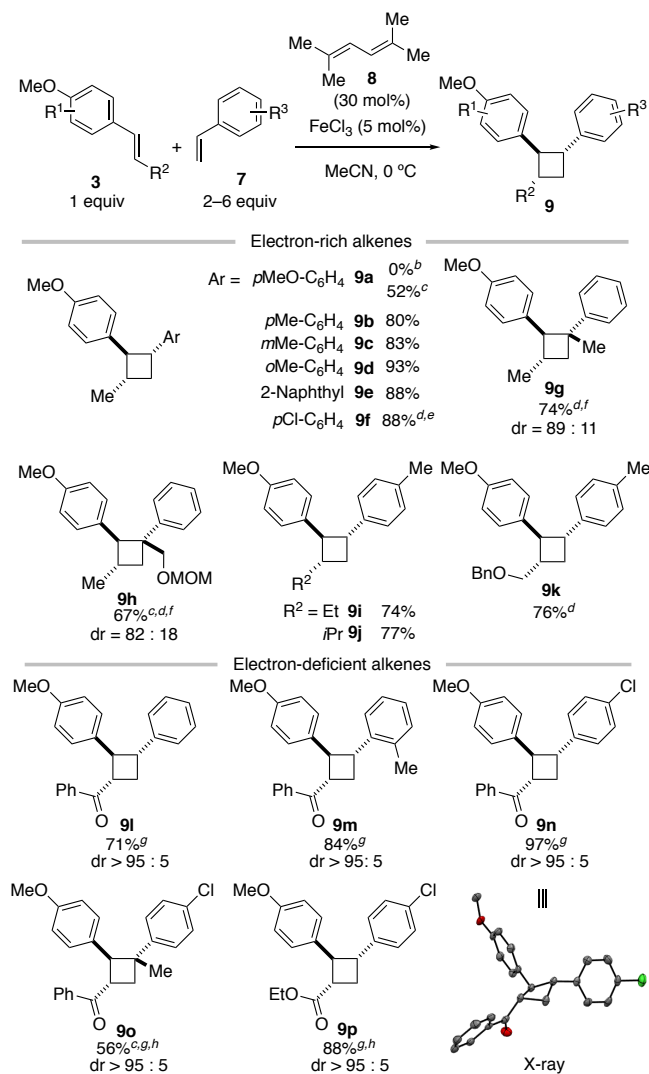
To test the synthetic potential of our approach, a large-scale reaction was conducted (Scheme 3). When 69.8 g of **3a** was reacted in the presence of 1 mol% of FeCl<sub>3</sub>, the crude product was obtained quantitatively in 2 h using a flask open to air. Moreover, removal of inorganic FeCl<sub>3</sub> by filtration through a short pad of silica-gel afforded pure **5a** in 95% yield (103.5 g), highlighting the operational simplicity of this methodology. Unlike photoredox catalysis, this method does not require specialized light-flux-maximizing flow apparatuses for large-scale reactions,<sup>26</sup> allowing FeCl<sub>3</sub>-initiated [4 + 2] cycloaddition to be conducted on a 100g scale in standard glassware.

**Scheme 3. 100-gram Scale Reaction.**



Next, we turned our attention to the cross [2 + 2] cycloaddition of **3** with **7** (Table 2). Initial attempts using **3a** with **7a** gave unsatisfactory results. Namely, the desired **9a** was not obtained because of a polymerization of **7a** and a degradation of **9a**. Nicewicz and coworker have previously reported a [2 + 2] cycloaddition in which a redox-mediator is employed as an additive to putatively accelerate the chain-propagation step and subsequently minimize such side reactions.<sup>27</sup> In a similar manner, we sought a redox-mediator. After screening of additives, diene **8** was found to suppress side reactions. When 5 mol% of FeCl<sub>3</sub> was used with 30 mol% of diene **8**, various substituted styrenes (**7a–7f**), which having electron-withdrawing and electron-donating groups on aromatics, gave the corresponding products in high yields (see **9a–9f**). Whereas there are only two examples of the use of  $\alpha$ -substituted styrenes in photoredox-initiated [2 + 2] cycloaddition,<sup>20a</sup>  $\alpha$ -substituted styrenes (see **9g** and **9h**) were also suitable substrates under our conditions. With respect to **3**, both a sterically-congested substituents and an allylic ether group on the olefin were well tolerated (see **9i–9k**). As above, in some cases (**9e**, **9g**, **9h** and **9k**), Fe(OTf)<sub>3</sub> was more effective than FeCl<sub>3</sub>.<sup>23</sup> To our delight, unprecedented electron-deficient **3** could be also used when Fe(OTf)<sub>3</sub> was employed. For examples, the corresponding products (**9l–9o**) were obtained in high yield with high diastereoselectivity when  $\alpha,\beta$ -unsaturated ketones with various styrenes were used. The major diastereomer of **9n** was unambiguously analyzed by X-ray crystallography. It is worth noting that  $\alpha$ -methyl substituted styrene also provided the corresponding **9o** in 56% yield with high diastereoselectivity. Moreover,  $\alpha,\beta$ -unsaturated esters could be well tolerated without a decrease in yield (see **9p**). In summary, iron(III) salt-initiated [2 + 2] cycloaddition exhibits high reactivity with a broad substrate scope of both electron-rich and electron-deficient alkenes.

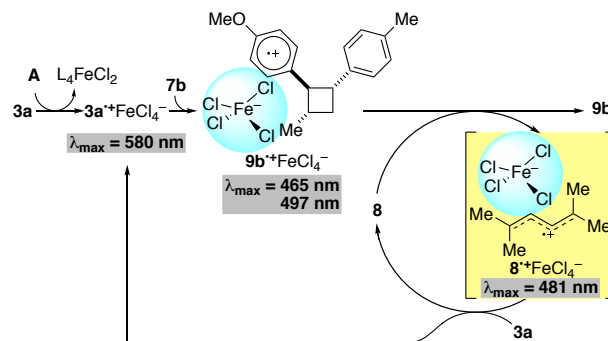
**Table 2. Scope of Radical Cation-induced [2 + 2] Cycloaddition.<sup>a</sup>**



<sup>a</sup>The reaction was carried out with  $\text{FeCl}_3$  (5 mol%), **3** (1 equiv) and **7** (2–6 equiv) in MeCN at 0 °C. <sup>b</sup>In the absence of **8**. <sup>c</sup>The yield was determined by <sup>1</sup>H NMR analysis using 1,3-dinitrobenzene as an internal standard. <sup>d</sup>Using  $\text{Fe}(\text{OTf})_3$  (5 mol%) instead of  $\text{FeCl}_3$ . <sup>e</sup>The reaction was carried out at room temperature. <sup>f</sup>The reaction was carried out at –20 °C. <sup>g</sup>Using  $\text{Fe}(\text{OTf})_3$  (10 mol%) instead of  $\text{FeCl}_3$ . <sup>h</sup>Using **8** (10 mol%).

To elucidate the role of **8** in [2 + 2] cycloaddition, UV-vis analyses were conducted (Figure S9 and S10). Upon UV-vis monitoring of the reaction of **9b**<sup>+</sup> with **8** (Figure S9), we observed the reduction of **9b**<sup>+</sup> ( $\lambda_{\text{max}} = 465 \text{ nm}$ ,  $497 \text{ nm}$ ) to give **9b** with concomitant formation of a new feature assigned to **8**<sup>+</sup> ( $\lambda_{\text{max}} = 481 \text{ nm}$ )<sup>28</sup>. Moreover, UV-vis observation of the reaction between **8**<sup>+</sup> and **3a** showed the generation of **3a**<sup>+</sup> ( $\lambda_{\text{max}} = 580 \text{ nm}$ ) along with **8** (Figure S10). These results suggest that **8** serves to promote the reduction of **9b**<sup>+</sup> and the subsequent oxidation of **3a** as a redox-mediator. The summarized mechanistic proposal is shown in Scheme 4. After the generation of **3a**<sup>+</sup> $\text{FeCl}_4^-$  by  $\text{FeCl}_3$ , [2 + 2] cycloaddition of **3a**<sup>+</sup> $\text{FeCl}_4^-$  with **7b** affords **9b**<sup>+</sup> $\text{FeCl}_4^-$ . The reduction of **9b**<sup>+</sup> $\text{FeCl}_4^-$  by **8** gives **9b** along with **8**<sup>+</sup> $\text{FeCl}_4^-$ . Subsequent oxidation of **3a** by **8**<sup>+</sup> $\text{FeCl}_4^-$  regenerates **3a**<sup>+</sup> $\text{FeCl}_4^-$  and **8**. As a result of accelerating the chain propagation step, side reactions might be suppressed (Figure S11).

#### Scheme 4. A Plausible Role of **8**.



In conclusion, the aromatic radical cation generated by  $\text{FeCl}_3$  has been isolated and characterized for the first time. Moreover, by virtue of the generation of the radical cation– $\text{FeCl}_4^-$  as an ion pair, radical cation-induced [4 + 2] cycloaddition and [2 + 2] cycloaddition were developed, with the latter leveraging a novel diene redox-mediator as a co-catalyst. In addition to delivering a mild, inexpensive, straightforward, and easily scalable method for radical cation-induced cycloaddition chemistry, these results shed new light on iron(III)-promoted single-electron chemistry writ large.

#### ASSOCIATED CONTENT

##### Supporting Information

The Supporting Information is available free of charge on the ACS Publications website at DOI: 10.1021/jacs.XXXXX.

Experimental procedure, characterization data, copies of <sup>1</sup>H NMR and <sup>13</sup>C NMR spectra of all new compounds (PDF)  
X-ray data for **2** and **9n** (CIF)

#### AUTHOR INFORMATION

##### Corresponding Author

\*E-mail: ishihara@cc.nagoya-u.ac.jp

##### ORCID

**Takahiro Horibe**: 0000-0002-4692-4642

**Kazuaki Ishihara**: 0000-0003-4191-3845

##### Notes

The authors declare no competing financial interest.

#### ACKNOWLEDGMENT

Financial support was partially provided by JSPS KAKENHI (Grant Numbers 15H05755, 15H05810, 15H06266 and 17K14484), Program for Leading Graduate Schools “IGER program in Green Natural Sciences”, Fuji-film Corporation Award in Synthetic Organic Chemistry, Japan and MEXT, Japan. We thank Mr. Kazuki Nishimura (Nagoya University) for his assistance with UV-vis spectrum analysis. Prof. Yoshihiro Miyake (Nagoya University) is acknowledged for helpful discussions on UV-vis analysis. We thank Dr. Mark D. Levin (Harvard University)

ty) for fruitful discussions and proofreading of the manuscript.

## REFERENCES

- (1) Linker, T. Cerium(IV) and other oxidizing agents, in *Radicals in Organic Synthesis*; Renaud, P.; Sibi, M. P. Eds.; Wiley: Weinheim, 2001; pp. 219–228.
- (2) For review of radical cation-induced reaction, see: Schmittel, M.; Burghart, A. Understanding Reactivity Patterns of Radical Cations. *Angew. Chem. Int. Ed.* **1997**, *36*, 2550.
- (3) Wang, X. Isolation and crystallization of radical cations by weakly coordinating anions, in *Organic Redox Systems: Synthesis, Properties, and Applications*, Nishinaga, T. Ed.; Wiley: New Jersey, 2015; pp. 523–544.
- (4) For a review of recent uses of FeCl<sub>3</sub>, see: Diaz, D. D.; Miranda, P. O.; Padrón, J. I.; Martin, V. S. Recent Uses of Iron(III) Chloride in Organic Synthesis. *Curr. Org. Chem.* **2006**, *10*, 457.
- (5) For reviews of iron-mediated oxidative coupling, see: (a) Sarhan, A. A. O.; Bolm, C. Iron(III) Chloride in Oxidative C–C Coupling Reactions. *Chem. Soc. Rev.* **2009**, *38*, 2730. (b) Jia, F.; Li, Z. Iron-catalyzed/mediated Oxidative Transformation of C–H Bonds. *Org. Chem. Front.* **2014**, *1*, 194.
- (6) For selected examples of oxidative coupling reactions, see: (a) Jempty, T. C.; Miller, L. L.; Mazur, Y. Oxidative Coupling Reactions Using Silica-bound Ferric Chloride. *J. Org. Chem.* **1980**, *45*, 749. (b) Jempty, T. C.; Gogins, K. A. Z.; Mazur, Y.; Miller, L. L. FeCl<sub>3</sub>/SiO<sub>2</sub> Reacts as Oxidant or Lewis Acid with Phenol Ethers. *J. Org. Chem.* **1981**, *46*, 4545. (c) Boden, N.; Bushby, R. J.; Lu, Z.; Headdock, G. Synthesis of Dibromotetraalkoxybiphenyls Using Ferric Chloride. *Tetrahedron Lett.* **2000**, *41*, 10117. (d) Siove, A.; Adès, D. Synthesis by Oxidative Polymerization with FeCl<sub>3</sub> of a Fully Aromatic Twisted Poly(3,6-carbazole) with a Blue-violet Luminescence. *Polymer* **2004**, *45*, 4045. (e) Wadumethrige, S. H.; Rathore, R. A Facile Synthesis of Elusive Alkoxy-substituted Hexa-*peri*-hexabenzocoronene. *Org. Lett.* **2008**, *10*, 5139. (f) Dou, C.; Saito, S.; Matsuo, K.; Hisaki, I.; Yamaguchi, S. A Boron-Containing PAH as a Substructure of Boron-Doped Graphene. *Angew. Chem. Int. Ed.* **2012**, *51*, 12206.
- (7) For review of Scholl reaction, see: Grzybowski, M.; Skonieczny, K.; Butenschön, H.; Gryko, D. T. Comparison of Oxidative Aromatic Coupling and the Scholl Reaction. *Angew. Chem. Int. Ed.* **2013**, *52*, 9900.
- (8) For selected examples of Scholl reaction, see: (a) Scholl, R.; Seer, C. Abspaltung Aromatisch gebundenen Wasserstoffs und Verknüpfung Aromatischer Kerne durch Aluminiumchlorid. *Justus Liebigs Ann. Chem.* **1912**, *394*, 111. (b) Fechtenkötter, A.; Saalwächter, K.; Harbison, M. A.; Müllen, K.; Spiess, H. W. Highly Ordered Columnar Structures from Hexa-*peri*-hexabenzocoronenes—Synthesis, X-ray Diffraction, and Solid-State Heteronuclear Multiple-Quantum NMR Investigations. *Angew. Chem. Int. Ed.* **1999**, *38*, 3039. (c) Ito, S.; Herwig, P. T.; Böhme, T.; Rabe, J. P.; Rettig, W.; Müllen, K. Bishexa-*peri*-hexabenzocoronenyli: A “Superbiphenyl”. *J. Am. Chem. Soc.* **2000**, *122*, 7698. (d) Wehmeier, M.; Wagner, M.; Müllen, K. Novel Perylene Chromophores Obtained by a Facile Oxidative Cyclodehydrogenation Route. *Chem. Eur. J.* **2001**, *7*, 2197. (e) Dou, X.; Yang, X.; Bodwell, G. J.; Wagner, M.; Enkelmann, V.; Müllen, K. Unexpected Phenyl Group Rearrangement during an Intramolecular Scholl Reaction Leading to an Alkoxy-Substituted Hexa-*peri*-hexabenzocoronene. *Org. Lett.* **2007**, *9*, 2485. (f) Luo, J.; Xu, X.; Mao, R.; Miao, Q. Curved Polycyclic Aromatic Molecules That Are  $\pi$ -Isoelectronic to Hexabenzocoronene. *J. Am. Chem. Soc.* **2012**, *134*, 13796.
- (9) For a review of polyphenylenes for material science, see: Berresheim, A. J.; Müller, M.; Müllen, K. Polyphenylene Nanostructures. *Chem. Rev.* **1999**, *99*, 1747.
- (10) For selected examples of radical cation-induced reaction by iron(III) salt, see: (a) Bell, F. A.; Crellin, R. A.; Fujii, H.; Ledwith, A. Cation-radicals: Metal-catalysed Cyclodimerisation of Aromatic Enamines. *J. Chem. Soc. D*, **1969**, 1969, 251. (b) Ohara, H.; Itoh, T.; Nakamura, M.; Nakamura, E. [2 + 2]-Cycloaddition Reaction of Styrene Derivatives Using an Fe(III) Salt Catalyst. *Chem. Lett.* **2001**, *30*, 624. (c) Cavanagh, C. W.; Aukland, M. H.; Hennessy, A.; Procter, D. J. Iron-mediated C–H Coupling of Arenes and Unactivated Terminal Alkenes Directed by Sulfur. *Chem. Commun.* **2015**, *51*, 9272.
- (11) (a) Meyer, S.; Koch, R.; Metzger, J. O. Investigation of Reactive Intermediates of Chemical Reactions in Solution by Electrospray Ionization Mass Spectrometry: Radical Cation Chain Reactions. *Angew. Chem. Int. Ed.* **2003**, *42*, 4700. (b) Marquez, C. A.; Wang, H.; Fabbretti, F.; Metzger, J. O. Electron-Transfer-Catalyzed Dimerization of *trans*-Anethole: Detection of the Distonic Tetramethylene Radical Cation Intermediate by Extractive Electrospray Ionization Mass Spectrometry. *J. Am. Chem. Soc.* **2008**, *130*, 17208.
- (12) Rathore, R.; Kochi, J. K. Isolation of Novel Radical Cations from Hydroquinone Ethers. Conformational Transition of the Methoxy Group upon Electron Transfer. *J. Org. Chem.* **1995**, *60*, 4399.
- (13) Gao, Y.; Guery, J.; Jacoboni, C. FeCl<sub>3</sub> Behavior in Acetonitrile: Structures of [FeCl<sub>2</sub>(CH<sub>3</sub>CN)<sub>4</sub>][FeCl<sub>4</sub>] and [AlCl(CH<sub>3</sub>CN)<sub>5</sub>][FeCl<sub>4</sub>]<sub>2</sub>·CH<sub>3</sub>CN. *Acta Cryst. C* **1993**, *49*, 147.
- (14) Dissociation of chloride from **A** is another possible rate-limiting step. To exclude this possibility, we conducted control experiments in the presence of chloride scavengers (see Table S1 in Supporting Information). However, chloride dissociation was not observed in these reactions. Therefore, dissociation of chloride and the generation of FeCl<sub>2</sub><sup>+</sup> are less likely.
- (15) Okada, Y.; Chiba, K. Redox-Tag Processes: Intramolecular Electron Transfer and Its Broad Relationship to Redox Reactions in General. *Chem. Rev.* **2018**, *118*, 4592.
- (16) (a) Bellville, D. J.; Bauld, N. L.; Pabon, R.; Gardner, S. A. Theoretical Analysis of Selectivity in the Cation-radical Diels–Alder. *J. Am. Chem. Soc.* **1983**, *105*, 3584. (b) Pabon, R. A.; Bellville, D. J.; Bauld, N. L. Cation Radical Diels–Alder Reactions of Electron-rich Dienophiles. *J. Am. Chem. Soc.* **1983**, *105*, 5158. (c) Reynolds, D. W.; Bauld, N. L. The Diene Component in the Cation Radical Diels–Alder. *Tetrahedron* **1986**, *42*, 6189. (d) Yueh, W.; Bauld, N. L. Mechanistic Aspects of Aminium Salt-Catalyzed Diels–Alder Reactions: the Substrate Ionization Step. *J. Phys. Org. Chem.* **1996**, *9*, 529.
- (17) (a) Lin, S.; Ischay, M. A.; Fry, C. G.; Yoon, T. P. Radical Cation Diels–Alder Cycloadditions by Visible Light Photocatalysis. *J. Am. Chem. Soc.* **2011**, *133*, 19350. (b) Stevenson, S. M.; Shores, M. P.; Ferreira, E. M. Photooxidizing Chromium Catalysts for Promoting Radical Cation Cycloadditions. *Angew. Chem. Int. Ed.* **2015**, *54*, 6506. (c) Higgins, R. F.; Fatur, S. M.; Shepard, S. G.; Stevenson, S. M.; Boston, D. J.; Ferreira, E. M.; Damrauer, N. H.; Rappé, A. K.; Shores, M.

P. Uncovering the Roles of Oxygen in Cr(III) Photoredox Catalysis. *J. Am. Chem. Soc.* **2016**, *138*, 5451. (d) Zhao, Y.; Antonietti, M. Visible-Light-Irradiated Graphitic Carbon Nitride Photocatalyzed Diels–Alder Reactions with Dioxygen as Sustainable Mediator for Photoinduced Electrons. *Angew. Chem. Int. Ed.* **2017**, *56*, 9336. (e) Stevenson, S. M.; Higgins, R. F.; Shores, M. P.; Ferreira, E. M. Chromium Photocatalysis: Accessing Structural Complements to Diels–Alder Adducts with Electron-deficient Dienophiles. *Chem. Sci.* **2017**, *8*, 654. (f) Higgins, R. F.; Fatur, S. M.; Damrauer, N. H.; Ferreira, E. M.; Rappé, A. K.; Shores, M. P. Detection of an Energy-Transfer Pathway in Cr-Photoredox Catalysis. *ACS Catal.* **2018**, *8*, 9216. (g) Morse, P. D.; Nguyen, T. M.; Cruz, C. L.; Nicewicz, D. A. Enantioselective Counter-anions in Photoredox Catalysis: The Asymmetric Cation Radical Diels–Alder Reaction. *Tetrahedron* **2018**, *74*, 3266.

(18) Okada, Y.; Yamaguchi, Y.; Ozaki, A.; Chiba, K. Aromatic “Redox Tag”-assisted Diels–Alder reactions by Electro-catalysis. *Chem. Sci.* **2016**, *7*, 6387.

(19) While we were preparing this manuscript, a related reports of radical cation-induced cycloaddition by iron(III) salt appeared. These describe the catalysis by iron(III) salt with O<sub>2</sub> for [4 + 2] cycloaddition and [2 + 2] cycloaddition: (a) Yu, Y.; Fu, Y.; Zhong, F. Benign Catalysis with Iron: Facile Assembly of Cyclobutanes and Cyclohexenes *via* Intermolecular Radical Cation Cycloadditions. *Green Chem.* **2018**, *20*, 1743. (b) Shin, J. H.; Seong, E. Y.; Mun, H. J.; Jang, Y. J.; Kang, E. J. Electronically Mismatched Cycloaddition Reactions *via* First-Row Transition Metal, Iron(III)–Polypyridyl Complex. *Org. Lett.* **2018**, *20*, 5872.

(20) (a) Ischay, M. A.; Ament, M. S.; Yoon, T. P. Crossed Intermolecular [2 + 2] Cycloaddition of Styrenes by Visible Light Photocatalysis. *Chem. Sci.* **2012**, *3*, 2807. (b) Li, R.; Ma, B. C.; Huang, W.; Wang, L.; Wang, D.; Lu, H.; Landfester, K.; Zhang, K. A. I. Photocatalytic Regioselective and Stereoselective [2 + 2] Cycloaddition of Styrene Derivatives Using a Heterogeneous Organic Photocatalyst. *ACS Catal.* **2017**, *7*, 3097.

(21) (a) Colomer, I.; Barcelos, R. C.; Donohoe, T. J. Catalytic Hypervalent Iodine Promoters Lead to Styrene Dimerization and the Formation of Tri- and Tetrasubstituted Cyclobu-

tanones. *Angew. Chem. Int. Ed.* **2016**, *55*, 4748. (b) Colomer, I.; Batchelor-McAuley, C.; Odell, B.; Donohoe, T. J.; Compton, R. G. Hydrogen Bonding to Hexafluoroisopropanol Controls the Oxidative Strength of Hypervalent Iodine Reagents. *J. Am. Chem. Soc.* **2016**, *138*, 8855.

(22) Triplet-sensitized cross [2 + 2] cycloadditions of  $\alpha,\beta$ -unsaturated carbonyls were recently reported. Variety of  $\alpha,\beta$ -unsaturated carbonyls can be used. However, diastereoselectivity is generally low because of *cis/trans* isomerization of  $\alpha,\beta$ -unsaturated carbonyls under photo irradiation conditions. (a) Miller, Z. D.; Lee, B. J.; Yoon, T. P. Enantioselective Crossed Photocycloadditions of Styrenic Olefins by Lewis Acid Catalyzed Triplet Sensitization. *Angew. Chem. Int. Ed.* **2017**, *56*, 11891. (b) Lei, T.; Zhou, C.; Huang, M.-Y.; Zhao, L.-M.; Yang, B.; Ye, C.; Xiao, H.; Meng, Q.-Y.; Ramamurthy, V.; Tung, C.-H.; Wu, L.-Z. General and Efficient Intermolecular [2 + 2] Photodimerization of Chalcones and Cinnamic Acid Derivatives in Solution through Visible-Light Catalysis. *Angew. Chem. Int. Ed.* **2017**, *56*, 15407.

(23) See Supporting Information for the results when FeCl<sub>3</sub> was used as an initiator.

(24) Cabrero-Antonino, J. R.; Leyva-Pérez, A.; Corma, A. Iron(III) Triflimide as a Catalytic Substitute for Gold(I) in Hydroaddition Reactions to Unsaturated Carbon–Carbon Bonds. *Chem. Eur. J.* **2013**, *19*, 8627.

(25) Yueh, W.; Bauld, N. L. Characterization of Cation Radical Reactions. Aminium Salt-catalysed Diels–Alder Reactions. *J. Chem. Soc., Perkin Trans. 2*, **1996**, 1761.

(26) Garlets, Z. J.; Nguyen, J. D.; Stephenson, C. R. J. The Development of Visible-light Photoredox Catalysis in Flow. *Isr. J. Chem.* **2014**, *54*, 351.

(27) Riener, M.; Nicewicz, D. A. Synthesis of Cyclobutane Lignans *via* an Organic Single Electron Oxidant–Electron Relay System. *Chem. Sci.* **2013**, *4*, 2625.

(28) Lew, C. S. Q.; Brisson, J. R.; Johnston, L. J. Reactivity of Radical Cations: Generation, Characterization, and Reactivity of 1,3-Diene Radical Cations. *J. Org. Chem.* **1997**, *62*, 4047.

